Available online at www.sciencedirect.com
ScienceDirect
Journal of Sound and Vibration 321 (2009) 620–630
JOURNAL OF SOUND AND VIBRATION
www.elsevier.com/locate/jsvi

Monitoring a deep hole drilling process by nonlinear time series modeling

Amor Messaoud*, Claus Weihs

Department of Statistics, Dortmund University of Technology, Germany

Received 17 July 2007; received in revised form 23 October 2008; accepted 26 October 2008
Handling Editor: A.V. Metrikine
Available online 20 December 2008

Abstract

Deep hole drilling methods are used for producing holes with a high length-to-diameter ratio, good surface finish and straightness. The process is subject to dynamic disturbances that is classified as either chatter vibration or spiralling. In this work, nonlinear time series modeling is used to setup an on-line modeling approach of the time varying dynamics of the process. An on-line monitoring strategy, based on control charts, is formed to detect chatter vibration. The results show that the proposed modeling approach provides an on-line procedure that can answer questions about the time varying dynamics of the process. The proposed on-line monitoring strategy can detect the start of the transition from stable drilling to chatter vibration and some alarm signals are related to changing physical conditions of the process.

1. Introduction

Deep hole drilling methods are used for producing holes with a high length-to-diameter ratio, good surface finish and straightness. For drilling holes with a diameter of 20 mm and above, the BTA (Boring and Trepanning Association) deep hole machining principle is usually employed. The process is subject to dynamic disturbances that is classified as either chatter vibration or spiralling. Chatter vibration leads to excessive wear of the cutting edges of the tool which has an undesirable effect on the tool life. In extreme cases, it damages the boring wall by causing marks, called chatter marks, on the cylindrical surface of the bore hole, see Fig. 1.

Concerning spiralling, it damages the workpiece severely. It leads to a multilobe-shaped deviation of the cross section of the hole from absolute roundness. The defect of shape and surface quality constitutes a significant impairment of the workpiece. Process reliability is of primary importance and disturbances should be avoided as the deep hole drilling process is often used during the last production phases of expensive workpieces. For example, axial bores in turbines or compressor shafts are made with this process.

The purpose of this work is to develop such real-time monitoring strategy to detect chatter vibration in order to allow the engineers to know when and how to adjust the process. For this reason, amplitude-dependent exponential autoregressive (ExpAr) time series models are used to describe the dynamics of the

*Corresponding author. Tel.: +49 231 7553755; fax: +49 231 7554387.
E-mail addresses: messaoud@statistik.uni-dortmund.de (A. Messaoud), weihs@statistik.uni-dortmund.de (C. Weihs).

0022-460X/$ - see front matter © 2008 Elsevier Ltd. All rights reserved.
doi:10.1016/j.jsv.2008.10.028

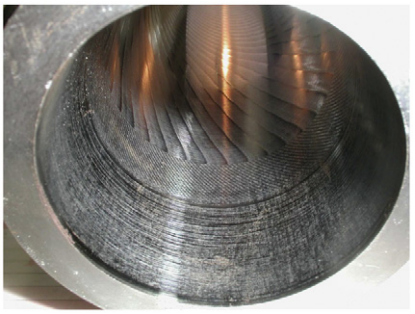

Fig. 1. Radial chatter marks.

process. This modeling approach provides the basis of an on-line monitoring strategy based on control charts. ExpAr time series modeling was used by Shi et al. [1] to detect machine tool chatter and by Shi et al. [2] to monitor the dynamics evolution of boiling water reactor (BWR) oscillation.

In Section 2, models that describe the time varying dynamics of the process are reviewed. In Sections 3 and 4, the ExpAr time series models and their estimation are discussed, respectively. In Section 5, ExpAr time series model-based control chats are proposed. In Section 6, the proposed monitoring strategy is applied to real data.

2. Nonlinear time varying process dynamics of the BTA deep hole drilling process

Several drilling experiments are conducted according to a given experimental design in order to study the dynamics of the process. The results show that using constant cutting parameters, time varying dynamics with alternating chatter and nonchatter phases is observed. Also, sudden changes of frequency during chatter phases occurred. During these experiments, several on-line measurements were sampled, see Weinert et al. [3]. Chatter is easily recognized in the on-line measurements by a fast increase of the dynamic part of the torque, force and acceleration signals. However, the drilling torque measurements yield the earliest and most reliable information about the transition from stable operation to chatter.

Weinert et al. [3] used dynamical systems to model the process. At a first stage, they are not interested in an exact and global modeling of all microscopic details of the drilling process, but only in a local description of adequate accuracy to predict disturbances sufficiently early and to provide insights into how to react in order to prevent them. Therefore, they proposed a phenomenological approach with a special emphasis on the temporal neighborhoods of instabilities or state transitions from stable drilling to chatter vibration and back.

The authors proposed a phenomenological model based on the van der Pol equation

$$\ddot{x}(t) + \varepsilon(b^2 - x(t)^2)\dot{x}(t) + w^2 x(t) = 0 \tag{1}$$

to describe the transition from stable drilling to chatter in one frequency. They have noted that the different kinds of solutions of Eq. (1) qualitatively coincide with the experimentally observed states in the drilling process. They have proposed to model the transition by a Hopf bifurcation in the van der Pol equation. Therefore, the drilling torque is described by

$$\ddot{x}(t) + \varepsilon(t)(b^2 - x(t)^2)\dot{x}(t) + w^2 x(t) = W(t), \tag{2}$$

where $x(t)$ is the drilling torque, b and w are constants, $\varepsilon(t)$ is a bifurcation parameter and $W(t)$ is a white noise process. Here w describes the behavior of a prominent frequency component at 703 Hz. $W(t)$ is included in order to model all the uncontrollable parameters of a drilling experiment as well as the microscopic details of the drilling process. In this case, Hopf bifurcation occurs in the system when a stable fixed point becomes unstable to form a limit cycle, as $\varepsilon(t)$ vary from positive to negative values. That is, the solution of Eq. (2)

changes from a stable fixed poind to a limit cycle as the process changes from stable drilling to chatter, respectively. Weinert et al. [3] elaborates the details and motivate the choice of this model.

3. Amplitude-dependent ExpAr time series models

ExpAr time series models are introduced by Ozaki and Oda [4] and Ozaki [5] in an attempt to reproduce certain features of nonlinear random vibration theory. They are able to reveal certain types of nonlinear dynamics such as fixed points and limit cycles. They have simple structure similar to autoregressive (AR) models except for the state-dependent coefficients. An ExpAr model is given by

$$x_t = (\phi_1 + \pi_1 \mathrm{e}^{-\gamma x_{t-1}^2})x_{t-1} + \cdots + (\phi_p + \pi_p \mathrm{e}^{-\gamma x_{t-1}^2})x_{t-p} + e_t, \tag{3}$$

where $\{e_t\}$ is a sequence of i.i.d. random variables, usually with zero mean and finite variance. γ, ϕ_i, π_i, $i = 1, \ldots, p$, are constants, where p is the model order. The nonlinearity of the process comes from the exponential form. This function renders the dynamics of the series locally to be linear but globally nonlinear. The AR coefficients are amplitude dependent. They change from $\phi_i + \pi_i$ to ϕ_i as $|x_{t-1}|$ changes from zero to $+\infty$. The nonlinear coefficient γ acts as a scaling factor. It modifies the effect of x_{t-1} in the term $\mathrm{e}^{-\gamma x_{t-1}^2}$.

Haggan and Ozaki [6] showed that the ExpAr model exhibit a limit cycle behavior under the following conditions:

(i) All the roots of the characteristic equation

$$\lambda^p - \phi_1\lambda^{p-1} - \phi_2\lambda^{p-2} - \cdots - \phi_p = 0 \tag{4}$$

lie inside the unit circle. Therefore x_t starts to damp out when $|x_{t-1}|$ becomes too large.

(ii) Some roots of the characteristic equation

$$\lambda^p - (\phi_1 + \pi_1)\lambda^{p-1} - (\phi_2 + \pi_2)\lambda^{p-2} - \cdots - (\phi_p + \pi_p) = 0 \tag{5}$$

lie outside the unit circle. Therefore, x_t starts to oscillate and diverge for small $|x_{t-1}|$.

The results of these two effects are expected to produce a sort of self-excited oscillation. The above two conditions are necessary for the existence of a limit cycle but not sufficient. A sufficient condition is

(iii)
$$\left(1 - \sum_{i=1}^{p} \phi_i\right) \Big/ \sum_{i=1}^{p} \pi_i > 1 \quad \text{or} \quad \left(1 - \sum_{i=1}^{p} \phi_i\right) \Big/ \sum_{i=1}^{p} \pi_i < 0. \tag{6}$$

Condition (iii) guarantees that a fixed point does not exist for the ExpAr model. Some ExpAr models without satisfying condition (iii) still have a limit cycle. Ozaki [7] noted that this is because the fixed points themselves of the model are unstable. The following condition is used to check whether the fixed points are stable or not whenever condition (iii) is not satisfied.

(iv) The fixed point of ExpAr model, if it exist, is stable if and only if the roots of the equation

$$\lambda^p - \beta_1\lambda^{p-1} - \beta_2\lambda^{p-2} - \cdots - \beta_p = 0 \tag{7}$$

lie inside the unit circle, where β_i's is given by

$$\beta_1 = \frac{\pi_1 + \phi_1 \sum_{j=1}^{p} \pi_j - \pi_1 \sum_{j=1}^{p} \phi_j}{\sum_{j=1}^{p} \pi_j} + 2\left(1 - \sum_{j=1}^{p} \phi_j\right) \log\left(\frac{1 - \sum_{j=1}^{p} \phi_j}{\sum_{j=1}^{p} \pi_j}\right),$$

$$\beta_i = \frac{\pi_i + \phi_i \sum_{j=1}^{p} \pi_j - \pi_i \sum_{j=1}^{p} \phi_j}{\sum_{j=1}^{p} \pi_j} \quad (i = 2, 3, \ldots, p). \tag{8}$$

4. Estimation of the ExpAr model

4.1. Maximum likelihood estimate

The maximum likelihood estimates of the parameters are obtained by minimizing the variance of the prediction errors, see Shi et al. [2]. Such estimation is, commonly, a time consuming nonlinear optimization procedure. Moreover, it can be proved that the objective function for the nonlinear coefficient γ is not convex where multiple local optima may exist. Therefore, there is no guarantee that a derivative-based method will converge to the global optimum. To overcome this problem, estimation procedures proposed by Haggan and Ozaki [6], Shi and Aoyama [8] and Baragona et al. [9] can be used. Haggan and Ozaki [6] proposed an approximate straightforward estimation method. First, a pre-specified interval for the γ value is fixed. This interval is divided into sub-intervals, so that a grid of candidates γ values is built. Then, the parameters $\{\phi_i, \pi_i\}$, $i = 1, 2, \ldots, p$, are estimated by linear least squares method on centered series. The order p of the fitted model is selected by use of the Akaike information criterion (AIC), see Haggan and Ozaki [6], given by

$$AIC(p) = (N - p)\log \hat{\sigma}_p^2 + 2(2p + 1), \tag{9}$$

where p is the order of the model to be considered, N is the total number of observations and $\hat{\sigma}_e^2$ is the least square estimate of the residual variance of the model.

Shi and Aoyama [8] and Baragona et al. [9] used a genetic algorithm to estimate the parameters of the model. However, for large values of $\{x_t\}$, the objective function may have a "golf-hole-like" problem, see Messaoud [10]. Genetic algorithms are not applicable to this kind of hard problems.

4.2. Real-time estimate

The previous estimation procedures involve computation difficulties and are not suitable for use in manufacturing systems (real-time), where CPU-time and memory are important. The main task of a real-time estimation procedure is the fast determination of the nonlinear coefficient γ. The estimation of the other coefficients $\{\phi_i, \pi_i\}$, $i = 1, 2, \ldots, p$, in the model is only a linear least squares problem whenever γ is determined. Shi et al. [2] proposed a heuristic determination of the nonlinear coefficient γ from the original data set,

$$\gamma_0 = -\frac{\log \delta}{\max x_i^2}, \tag{10}$$

where δ is a small number (i.e., $\delta = 0.0001$), $1 \leqslant i < N$ and N is the length of the data series. The idea behind this setting is that the model coefficients can approach constants values ϕ_i or $\phi_i + \pi_i$ if the observation moves far away from equilibrium or zero, respectively. The ExpAr model will definitely reveal the limit cycle behavior of underlying time series by fixing $\gamma = \gamma_0$ even it is not an optimum condition.

5. ExpAr time series based control charts

5.1. Introduction to control charts

Process variation is inevitable and can be classified as either common causes of variation or special causes of variation. Common or chance causes of variation are considered to be due to the inherent nature of the process and cannot be altered without changing the process itself. Assignable or special causes of variation are unusual shocks or other disruptions to the process. These causes can and should be removed. A process is said to be in a state of statistical control if it operates under common causes of variation and the probability distribution representing the quality characteristic is constant over time. If there are some changes over time in this distribution, the process is said to be out of control.

Control charts are used to detect the presence of assignable causes of variation so that corrective actions, if necessary, can be taken as soon as possible. Fig. 2 shows a typical Shewhart $\overline{X}$ control chart. It is one of the most frequently used statistical process control tools. Samples are taken at equally spaced intervals. Control

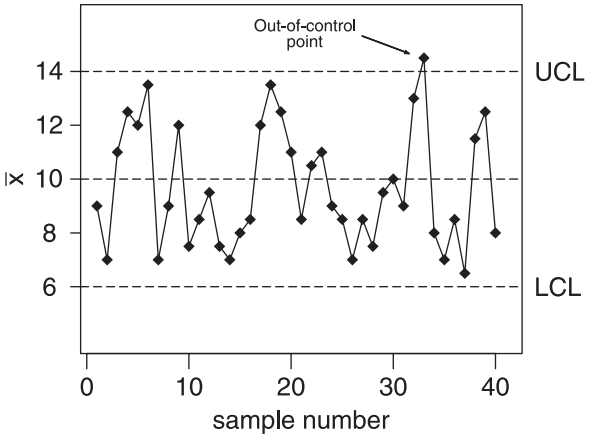

Fig. 2. An illustration of a Shewhart control chart (UCL: upper control limit and LCL: lower control limit).

statistic $\overline{X}$ of each sample, meant to summarize process behavior at the period in question, is computed and plotted against time.

As long as the plotted points remain inside the control limits, it is assumed that the process is in state of statistical control. An out-of-control signal is given by the chart as soon as a point falls outside the upper and lower control limits, labelled UCL and LCL, respectively.

Shewhart $\overline{X}$ control charts use only the current observation or sample to monitor the process. Other control charts, such as cumulative sum (CUSUM) and exponentially weighted moving average (EWMA) charts, accumulate information across successive observations. That is, they not only use the current sample statistic, but incorporate the information that can be gained from the previous sample statistics in some fashion. For further details, see Montgomery [11].

A basic assumption, used in the development of many control charts, is that the underlying distribution of the process is normal. The statistical properties of these charts are exact only if this assumption is satisfied. In practice, it is well known that this assumption rarely holds. Therefore, distribution-free or nonparametric control charts are used. For further details, see Chakraborti et al. [12].

5.2. The proposed control charts

In this work, ExpAr time series based control charts are proposed. Usually, time series based control charts are used to monitor the residuals, where a time series model is used to fit the data and to calculate the residuals. However, the drilling process is characterized by large amounts of data and therefore residuals, see Section 6.1. This causes the inapplicability of monitoring the residuals. Therefore, monitoring the parameters $\hat{\sigma}_e^2$ and $\hat{\gamma}$ of the estimated ExpAr time series models is considered.

In the following, let $r\text{EWMA}^{\hat{\sigma}}$ and $r\text{EWMA}^{\hat{\gamma}}$ refer to the nonparametric EWMA control charts based on sequential ranks that are used to monitor $\{\hat{\sigma}_{e,t}^2\}$ and $\{\hat{\gamma}_t\}$, $t = 1, 2, \ldots$, respectively. These charts were proposed by Hackl and Ledolter [13].

At time t, $RS^{\hat{\sigma}} = \{\hat{\sigma}_{e,t-m+1}^2, \ldots, \hat{\sigma}_{e,t}^2\}$ and $RS^{\hat{\gamma}} = \{\hat{\gamma}_{t-m+1}, \ldots, \hat{\gamma}_t\}$ denote the reference samples composed of $m > 1$ most recent estimated values of σ_e^2 and γ. They are used to decide whether or not the process is still in-control at time t. Note that the monitoring procedure starts at $t = m$. The sequential rank of $\hat{\sigma}_{e,t}^2$ among $RS^{\hat{\sigma}}$ is given by

$$Q_{\hat{\sigma},t}^{*} = 1 + \sum_{i=t-m+1}^{t} I(\hat{\sigma}_{e,t}^2 > \hat{\sigma}_{e,i}^2), \tag{11}$$

where $I(\cdot)$ is the indicator function. Similarly, the sequential rank of $\hat{\gamma}_t$ among $RS^{\hat{\gamma}}$ is given by

$$Q_{\hat{\gamma},t}^{*} = 1 + \sum_{i=t-m+1}^{t} I(\hat{\sigma}_{e,t}^2 > \hat{\sigma}_{e,t}^2). \tag{12}$$

$Q^*_{\hat{\sigma},t}$ and $Q^*_{\hat{\gamma},t}$ are uniformly distributed on the m points $\{1,2,\ldots,m\}$. The standardized sequential rank Q^m_t is given by

$$Q^m_{\hat{\sigma},t} = \frac{2}{m}\left(Q^*_{\hat{\sigma},t} - \frac{m+1}{2}\right) \quad \text{and}$$

$$Q^m_{\hat{\gamma},t} = \frac{2}{m}\left(Q^*_{\hat{\gamma},t} - \frac{m+1}{2}\right). \tag{13}$$

They are uniformly distributed on the m points

$$\left\{\frac{1}{m} - 1, \frac{3}{m} - 1, \ldots, 1 - \frac{1}{m}\right\} \tag{14}$$

with mean $\mu_{Q^m_t} = 0$ and variance $\sigma_{Q^m_t} = (m^2-1)/3m^2$. For more details, see Hackl and Ledolter [13].

For the $r\text{EWMA}^{\hat{\sigma}}$ control chart, the control statistic $T_{\hat{\sigma},t}$ is the EWMA of standardized sequential ranks. It is computed as follows:

$$T_{\hat{\sigma},t} = \max\{A, (1-\lambda_{\hat{\sigma}})T_{\hat{\sigma},t-1} + \lambda_{\hat{\sigma}} Q^m_{\hat{\sigma},t}\}, \tag{15}$$

$t = 1,2,\ldots$, where $0 < \lambda_{\hat{\sigma}} \leqslant 1$ is a smoothing parameter, A is a lower reflection boundary and $T_{\hat{\sigma},0}$ is a starting value usually set equal to 0. The process is considered in-control as long as $T_{\hat{\sigma},t} \leqslant h_{\hat{\sigma}}$, where $h_{\hat{\sigma}} > 0$ is an upper control limit. Note that the upper-sided $r\text{EWMA}^{\hat{\sigma}}$ control chart is considered because the statistic $Q^m_{\hat{\sigma},t}$ is "lower the better". Indeed, a decrease in $\hat{\sigma}^2_{e,t}$ means a process improvement.

For the $r\text{EWMA}^{\hat{\gamma}}$ control chart, the control statistic $T_{\hat{\gamma},t}$ is given by

$$T_{\hat{\gamma},t} = \min\{B, (1-\lambda_{\hat{\gamma}})T_{t-1} + \lambda_{\hat{\gamma}} Q^m_{\hat{\gamma},t}\}, \tag{16}$$

$t = 1,2,\ldots$, where $0 < \lambda_{\hat{\gamma}} \leqslant 1$ is a smoothing parameter, B is an upper reflection boundary and $T_{\hat{\gamma},0}$ is a starting value usually set equal to 0. The process is considered in-control as long as $T_{\hat{\gamma},t} \geqslant h_{\hat{\gamma}}$, where $h_{\hat{\gamma}} < 0$ is a lower control limit. Note that the lower-sided $r\text{EWMA}^{\hat{\gamma}}$ control chart is considered because the statistic $Q^m_{\hat{\gamma},t}$ is "higher the better". Indeed, an increase in $\hat{\gamma}_t$ means a process improvement.

The parameters of the two control charts are selected according to a performance criterion of the charts. Usually, the performance of control charts are evaluated by the average run length (ARL). The run length is defined as the number of observations that are needed to exceed the control limit for the first time. The ARL should be large when the process is statistically in-control, in-control ARL, and small when a shift has occurred, out-of-control ARL.

6. Monitoring the BTA deep hole drilling process

6.1. Modeling the nonlinear time varying dynamics of the process using ExpAr time series models

In this section, ExpAr time series models are used to describe the evolution of the drilling torque and to characterize the time varying dynamics of the process in an experiment with a feed $f = 0.120\,\text{mm}$, a cutting speed of $v_c = 90\,\text{m}\,\text{min}^{-1}$ and an amount of oil of $\dot{V}_{oil} = 300\,\text{l}\,\text{min}^{-1}$. The data are recorded with a sampling rate of $S = 20\,000\,\text{Hz}$ and consist of 10 506 240 observations that are shown in Fig. 3. This experiment is the most stable experiment of the experimental design and only slight chatter marks are observed on the bore hole wall at the end of process after depth 400 mm. This may be explained by the low cutting speed used.

A common way to solve the problem of on-line monitoring of the drilling process is to segment on-line measurements of the drilling torque, where it becomes very important to achieve a fast decision-making about the dynamics of the process through inference and analysis of the estimated ExpAr models in each segment. The data are divided into segments of length 4096 observations, which is used by Theis [14] to calculate the periodograms. In each segment, the ExpAr(p) time series model, given by Eq. (3), is fitted to centered data. The parameters are estimated using the real-time estimation procedure with $\delta = 0.0001$ in Eq. (10). The choice of a proper model order p is not an easy task. Fig. 4 shows the AIC criterion for two time series segments before and after chatter. The decrease of AIC criterion as p increases may be explained by the autocorrelation

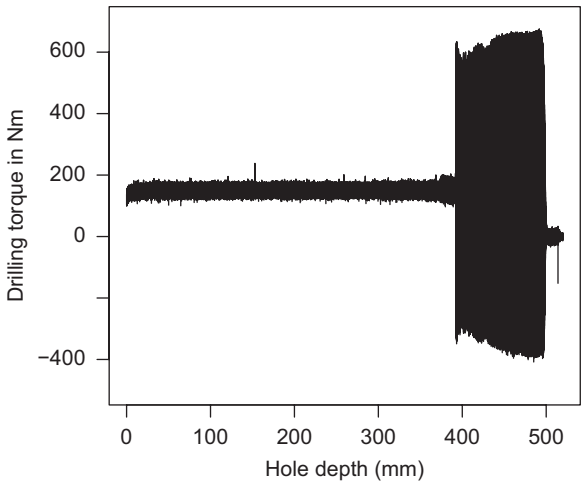

Fig. 3. Time series of the drilling torque.

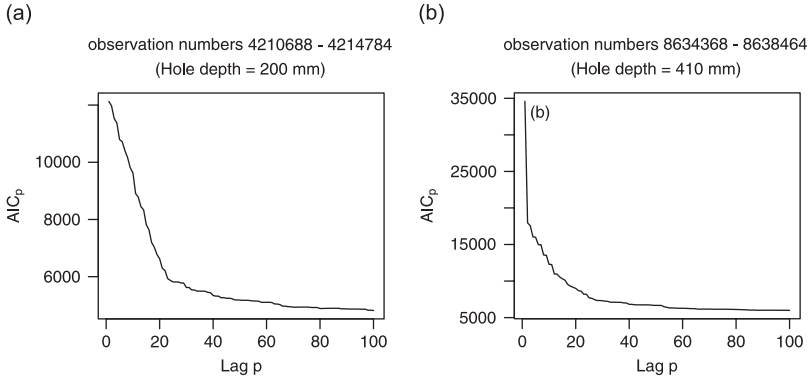

Fig. 4. AIC criterion of two time series segments: (a) before chatter and (b) after chatter.

function. Fig. 5 shows the autocorrelation function for the two time series segments. It shows that for the first segment the autocorrelation decreases as p increases. For the second segment, the autocorrelation shows the existence of a periodic behavior. A time lag $p = 40$ is selected. It is a reasonable choice but not optimal. In practice, it is easy to justify the use of a model with 81 parameters for 4096 observations. Moreover, the nature of collected data in this process, "data rich" problems in industry, justifies the use of such models.

For model diagnostic, the residuals are plotted against hole depth in mm in Fig. 6. Note that there is a slight increase in the variance of the residuals after depth 400 mm, which is during chatter vibration. This increase is clear in Fig. 7 where the least square estimate of the residual variance, $\hat{\sigma}_{\varepsilon}^2$, of the model is plotted with the hole depth in mm. Fig. 8 shows the histograms of the errors over two segments during stable drilling and chatter. They have a symmetric shape around zero and Gaussian appearance. As a final check, the fitted model is simulated using the estimated coefficients and residual variance. The first $p = 40$ values of the drilling torque in each segment are used as initial values. In fact, a model which cannot reproduce a similar series by simulation is certainly not interesting to statisticians and engineers. The results show that the simulated values behave similar to the observed data. In conclusion, the estimated ExpAr(40) model provides a good fit to the drilling torque measurements.

An important question is whether the ExpAr(40) time series model describes the nonlinear time varying dynamics of the process, see Section 2. In Section 3, it is mentioned that the ExpAr model exhibits the limit

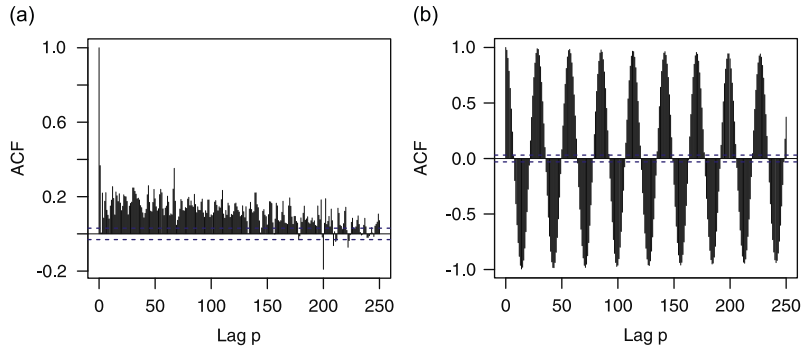

Fig. 5. Autocorrelation function of two time series segments: (a) before chatter and (b) after chatter.

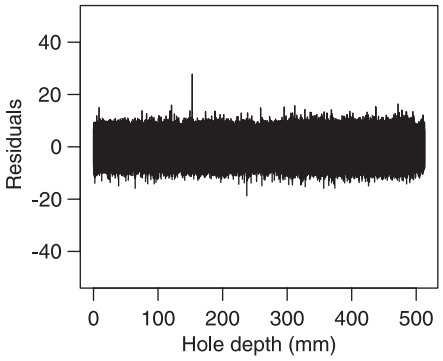

Fig. 6. Plot of the residuals.

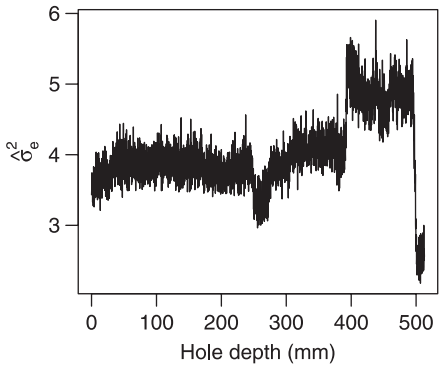

Fig. 7. The least square estimate of the residual variance, $\hat{\sigma}_e^2$.

cycle behavior under some conditions. These conditions are checked in each data segment. Fig. 9 shows the results. It is clear that these conditions are satisfied after depth 400 mm, during chatter vibration. This result is obvious for engineers, and Weinert et al. [3] used it to propose the model that describes the transition from stable drilling to chatter, see Section 2. In fact, it is known that machine tool chatter is a nonlinear oscillation of the limit cycle type, which can be regarded as an intrinsic property independent of process working conditions and measuring noise, see Tobias [15].

As a conclusion, the use of the ExpAr(40) time series model provides an on-line procedure that can be used to answer questions about the nonlinear time varying dynamics of the process. Its real-time implementation can be guaranteed. Furthermore, it can be used to decide whether the process is stable or not.

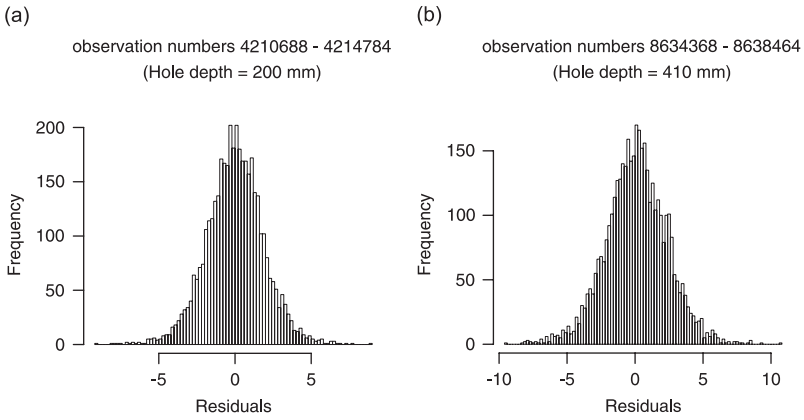

Fig. 8. Histograms of the residuals: (a) before chatter and (b) after chatter.

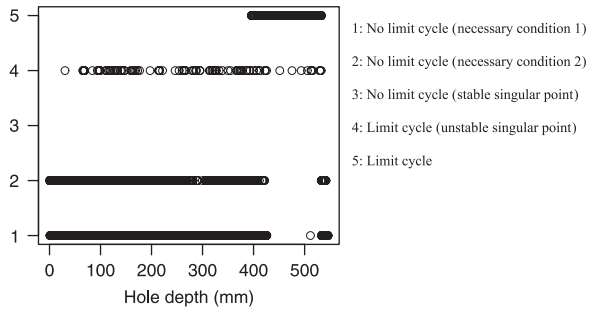

Fig. 9. Description of the time varying dynamics of the drilling torque.

6.2. Monitoring the process: experimental results

In this section, the estimated values of σ_e^2 and γ, see Section 6.1, are monitored using different $r\text{EWMA}^{\hat{\sigma}}$ and $r\text{EWMA}^{\hat{\gamma}}$ control charts. The parameters of these charts are selected so that they have the same in-control ARL equal to 370. This choice should avoid excessive false alarm signals because all control charts are applied to 2000 observations. The values 0.1, 0.3 and 0.5 are chosen for the smoothing parameters $\lambda_{\hat{\sigma}}$ and $\lambda_{\hat{\gamma}}$. Table 1 gives the values of $h_{\hat{\sigma}}$, $h_{\hat{\gamma}}$, A and B.

Note that the control limits are adjusted using simulations, see Messaoud [10]. The standardized sequential ranks are calculated with respect to the $m = 100$ recent observations, $\hat{\sigma}^2_{e,t-100}, \ldots, \hat{\sigma}^2_{e,t-1}$. For further details about the motivation of this choice see Messaoud [10].

Table 2 shows the results for depth $\leqslant$ 400 mm. First, the ability of the different control charts to quickly detect the known changes in the dynamics of the process is investigated. Table 2 shows that the control charts, except the $r\text{EWMA}^{\hat{\sigma}}$ ($\lambda_{\hat{\sigma}} = 0.5$) control chart, produce many out-of-control signals at 32 $\leqslant$ depth $\leqslant$ 50 mm. In fact, it is known that approximately at depth = 32 mm the guiding pads of the BTA tool leave the starting bush. This induces a sudden change in the dynamics of the process caused by the tool being freed. From previous experiments, the process has been observed to either stay stable or start with chatter vibration. The second known change in the dynamics of the process occurs approximately at depth 110 mm. It is the position where the tool enters the bore hole completely. Theis [14] noted that this might lead to changes in the dynamics of the process because the boring bar is slightly thinner than the tool and therefore the pressures in the hole may change. The $r\text{EWMA}^{\hat{\sigma}}$ ($\lambda_{\hat{\sigma}} = 0.1$) and $r\text{EWMA}^{\hat{\gamma}}$ ($\lambda_{\hat{\gamma}} = 0.1$ and 0.3) control charts detect this change and signal at 100 $\leqslant$ depth $\leqslant$ 125 mm.

Messaoud [10] showed that a change in the boundary conditions occurs approximately after depth 250 mm. The three $r\text{EWMA}^{\hat{\sigma}}$ control charts produce many out-of-control signals. However, the $r\text{EWMA}^{\hat{\gamma}}$ did not

Table 1
Adjusted control limits of the $r\text{EWMA}^{\hat{\sigma}}$ and $r\text{EWMA}^{\hat{\gamma}}$ control charts.

	$r\text{EWMA}^{\hat{\sigma}}$ $\lambda_{\hat{\sigma}}$			$r\text{EWMA}^{\hat{\gamma}}$ $\lambda_{\hat{\gamma}}$		
	0.10	0.30	0.50	0.10	0.30	0.50
Control limit	0.318	0.593	0.756	−0.318	−0.593	−0.756
Reflection boundary	−0.318	−0.593	−0.756	0.318	0.593	0.756

Table 2
Out-of-control signals of the different control charts.

Hole depth (mm)	$r\text{EWMA}^{\hat{\sigma}}$ $\lambda_{\hat{\sigma}}$			$r\text{EWMA}^{\hat{\gamma}}$ $\lambda_{\hat{\gamma}}$		
	0.1	0.3	0.5	0.1	0.3	0.5
⩽32	0	0	0	0	0	0
32–50	39	7	0	21	4	2
50–75	0	0	0	0	0	0
75–100	0	0	0	0	0	0
100–125	1	0	0	6	1	0
125–150	0	0	0	2	2	1
150–175	0	0	0	4	1	0
175–200	0	0	0	0	0	0
200–225	0	0	0	0	0	0
225–250	0	0	0	0	0	0
250–275	12	8	3	0	0	0
275–300	72	37	13	13	4	3
300–325	53	21	8	12	4	2
325–350	1	0	0	0	0	0
350–375	0	1	1	25	11	9
375–400	38	38	30	91	50	30

produce any signal. A second change in the dynamics of the process is observed at $275 \leqslant \text{depth} \leqslant 350$ mm, see Messaoud [10]. This explains the observed out-of-control signals at $275 \leqslant \text{depth} \leqslant 350$ mm. The transition from stable drilling to chatter vibration starts approximately after depth 350 mm. All control charts detect this start of transition and many out-of-control signals are produced until depth 400 mm. Note that the $r\text{EWMA}^{\hat{\sigma}}$ ($\lambda_{\hat{\sigma}} = 0.1$) produces an early out-of-control signal at 342 mm and more out-of-control signals are produced by the $r\text{EWMA}^{\hat{\gamma}}$ than $r\text{EWMA}^{\hat{\sigma}}$ control charts as well. In this experiment chatter vibration may be avoided if corrective actions are taken after these signals.

Table 2 shows that only nine out-of-control signals are produced by the $r\text{EWMA}^{\hat{\gamma}}$ control charts at $125 \leqslant \text{depth} \leqslant 175$ mm. These signals are not explained by any known change in the dynamics of the process. Note that a successful monitoring procedure should produce few false alarms during stable drilling in order to avoid unnecessary process adjustments.

As a conclusion, the results show that the proposed monitoring strategy quickly detect the start of the transition from stable drilling to chatter vibration in the considered experiment. That is, chatter may be avoided if corrective actions are taken after these signals. Furthermore, most of the out-of-control signals produced by the different control charts are related to known changes in the dynamics of the process. Furthermore, the performance of the proposed monitoring strategy is investigated using data sets from six experiments, see Messaoud [10]. The results show that the proposed control charts detect the start of the transition from stable drilling to chatter vibration. However, in some experiments they produce many

out-of-control signals that are not related to known changes in the dynamics of the process. This may be due to the "nonoptimal" estimation procedure of γ and choice of the time lag $p = 40$ of the ExpAr time series models.

In this work, the values 0.1, 0.3 and 0.5 are considered for the smoothing parameters $\lambda_{\hat{\sigma}}$ and $\lambda_{\hat{\gamma}}$ of the $r\text{EWMA}^{\hat{\sigma}}$ and $r\text{EWMA}^{\hat{\gamma}}$, respectively. However, in practice a procedure to choose these parameters is needed.

7. Conclusion

The main objective of this work is to develop an on-line monitoring strategy of the BTA deep hole drilling process. This work shows that ExpAr time series models can be used to setup an on-line modeling approach of the time varying dynamics of the process. This modeling approach provides the basis of an on-line monitoring strategy based on control charts. The results show that it can detect the start of the transition from stable drilling to chatter vibration and that some out-of-control signals are related to changing physical conditions of the process (i.e., guiding pads leave the starting bush, the tool is completely in the hole).

Acknowledgments

This work has been supported by Collaborative Research Centre "Reduction of Complexity in Multivariate Data Structures" (SFB 475) of the German Research Foundation (DFG). The authors would like to thank the editor and the referees for making many helpful comments and suggestions on earlier versions of this article.

References

[1] Z. Shi, Y. Tamura, T. Ozaki, A study on real-time detecting of machine tool chatter, *International Journal of the Japan Society for Precision Engineering* 32 (1998) 178–182.
[2] Z. Shi, Y. Tamura, T. Ozaki, Monitoring the stability of BWR oscillation by nonlinear time series modelling, *Annals of Nuclear Energy* 28 (2001) 953–966.
[3] K. Weinert, O. Webber, M. Hüsken, J. Mehnen, W. Theis, Analysis and prediction of dynamic disturbances of the BTA deep hole drilling process, in: R. Teti (Ed.), *Proceedings of the Third CIRP International Seminar on Intelligent Computation in Manufacturing Engineering*, ICME, 2002, Ischia, Italy, pp. 297–302.
[4] T. Ozaki, H. Oda, Nonlinear time series model identification by Akaike's information criterion, in: B. Dubuisson (Ed.), *Information and Systems*, Pergamon Press, Oxford, New York, 1978, pp. 83–91.
[5] T. Ozaki, Non-linear time series models for non-linear random vibrations, *Journal of Applied Probability* 17 (1980) 84–93.
[6] V. Haggan, T. Ozaki, Modelling nonlinear random vibrations using an amplitude-dependent autoregressive time series model, *Biometrika* 68 (1981) 189–196.
[7] T. Ozaki, The statistical analysis of perturbed limit cycle processes using nonlinear time series models, *Journal of Time Series Analysis* 3 (1982) 29–41.
[8] Z. Shi, H. Aoyama, Estimation of the exponential autoregresive time series model by using the genetic algorithm, *Journal of Sound and Vibration* 205 (1997) 309–321.
[9] R. Baragona, F. Battaglia, D. Cucina, A note on estimating autoregressive exponential models, *Quaderni di Statistica* 4 (2002) 71–88.
[10] A. Messaoud, Monitoring Strategies for Chatter Detection in a Drilling Process, PhD Thesis, Department of Statistics, University of Dortmund, 2006 ⟨http://hdl.handle.net/2003/23274⟩.
[11] D.C. Montgomery, *Introduction to Statistical Quality Control*, fourth ed., Wiley, New York, NY.
[12] S. Chakraborti, P. Van der Laan, S.T. Bakir, Nonparametric control charts: an overview and some results, *Journal of Quality Technology* 33 (2001) 304–315.
[13] P. Hackl, J. Ledolter, A new nonparametric quality control technique, *Communications in Statistics—Simulation and Computation* 21 (1992) 423–443.
[14] W. Theis, Modelling Varying Amplitudes, PhD Thesis, Department of Statistics, University of Dortmund, 2004.
[15] S.A. Tobias, *Machine Tool Vibration*, Blackie and Sons Ltd., London, 1965.